JCI insight

Tubular injury triggers podocyte dysfunction by β-catenin-driven release of MMP7

Roderick J. Tan, Yingjian Li, Brittney M. Rush, Débora Malta Cerqueira, Dong Zhou, Haiyan Fu, Jacqueline Ho, Donna Beer Stolz, Youhua Liu

JCI Insight. 2019. https://doi.org/10.1172/jci.insight.122399.

Research In-Press Preview Nephrology

Graphical abstract

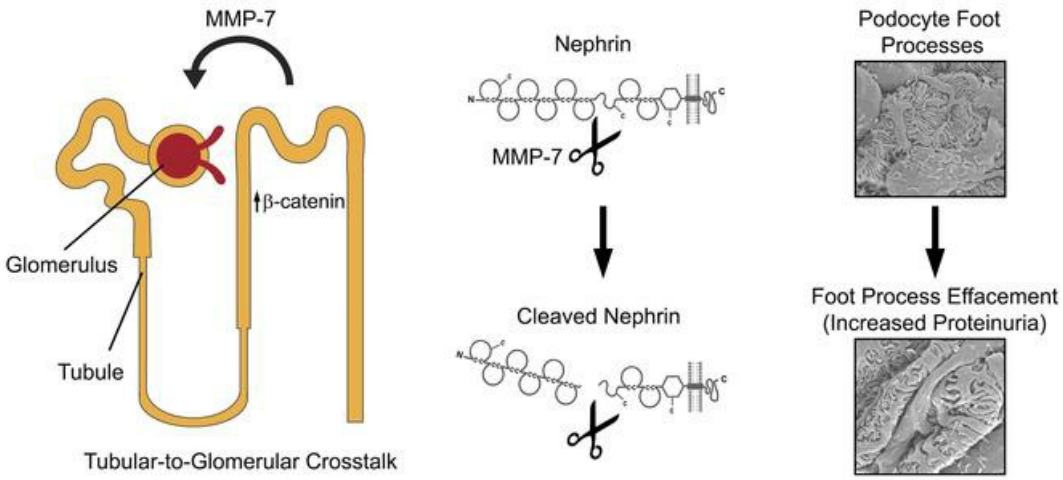

Tubular injury triggers podocyte dysfunction by β-catenin-driven release of MMP-7

Roderick J. Tan[1], Yingjian Li[2], Brittney M. Rush[1], Débora Malta Cerqueira[3], Dong Zhou[2], Haiyan Fu[4], Jacqueline Ho[3], Donna Beer Stolz[5], and Youhua Liu[2,4]

[1]Renal-Electrolyte Division, Department of Medicine, [2]Department of Pathology, [3]Division of Pediatric Nephrology, Department of Pediatrics, University of Pittsburgh School of Medicine, Pittsburgh, PA; [4]Division of Nephrology, Nanfang Hospital, Southern Medical University, Guangzhou, China; [5]Department of Cell Biology, University of Pittsburgh School of Medicine, Pittsburgh, PA.

Running Title: Tubular MMP-7 Enhances Proteinuria

Abstract: 198

Word count: 6,176

To whom correspondence should be addressed:

Roderick Tan, M.D., Ph.D., Department of Medicine, Renal-Electrolyte Division, 828A Scaife Hall, 3550 Terrace Street, Pittsburgh, PA 15261. Phone: (412) 624-4008. Fax: (412) 647-6222. Email: TANRJ@upmc.edu; and Youhua Liu, Ph.D, Department of Pathology, University of Pittsburgh, S-405 Biomedical Science Tower, 200 Lothrop Street, Pittsburgh, PA 15261. Phone: (412) 648-8253. Fax: (412) 648-1916. E-mail: yhliu@pitt.edu

ABSTRACT

Proteinuric chronic kidney disease (CKD) remains a major health problem worldwide. While the progression of primary glomerular disease to induce tubulointerstitial lesions is well established, the effect of tubular injury to trigger glomerular damage is poorly understood. We hypothesized that injured tubules secrete mediators that adversely affect glomerular health. To test this, we utilized conditional knockout mice with tubule-specific ablation of β-catenin (Ksp-β-cat-/-), and subjected them to chronic angiotensin II (Ang II) infusion or adriamycin. Compared to control mice, Ksp-β-cat-/- mice were dramatically protected from proteinuria and glomerular damage. Matrix metalloproteinase-7 (MMP-7), a downstream target of β-catenin, was upregulated in treated control mice, but this induction was blunted in the Ksp-β-cat-/- littermates. Incubation of isolated glomeruli with MMP-7 *ex vivo* led to nephrin depletion and impaired glomerular permeability. Furthermore, MMP-7 specifically and directly degraded nephrin in cultured glomeruli or cell-free systems, and this effect was dependent on its proteolytic activity. *In vivo,* expression or infusion of exogenous MMP-7 caused proteinuria, and genetic ablation of MMP-7 protected mice from Ang II-induced proteinuria and glomerular injury. Collectively, these results demonstrate that β-catenin-driven MMP-7 release from renal tubules promotes glomerular injury via direct degradation of the key slit diaphragm protein nephrin.

Keywords

Chronic kidney disease, proteinuria, MMP-7, nephrin, podocyte, angiotensin

INTRODUCTION

Chronic kidney disease (CKD), or the permanent loss of renal function, is a growing health concern. In the United States alone CKD affects more than 35 million individuals (1). In particular, CKD characterized by abnormal urinary protein excretion (proteinuria) carries a high risk of progression to end-stage renal disease (ESRD) (2). Unfortunately, treatment for proteinuric CKD remains extremely limited. In this context, a better understanding of the underlying pathologic mechanisms is essential for developing more effective therapies for CKD.

Regardless of the initial etiology, CKD progression to ESRD is characterized by increasingly widespread lesions in different compartments of kidney parenchyma. While diseases that primarily affect the glomerular compartment of the nephron (e.g. glomerulonephritis) are known to lead eventually to tubular injury and interstitial fibrosis (3), whether and how tubular injury affects the glomerular compartment are less well established and poorly understood. Studies show that kidney tubules can affect glomerular biology via signals originating from the macula densa, a specialized portion of the thick ascending limb of the loop of Henle (4). Considering the close apposition of renal tubules to glomeruli, it is possible that tubules influence glomerular health in other ways. Interestingly, in a model of acute kidney injury (AKI) that specifically targeted renal tubules, Grgic et al. found that approximately 20% of the glomeruli developed sclerotic lesions (5). This was accompanied by an increase in proteinuria and suggested a significant tubular effect on glomerular health. However, the underlying mechanism by which tubular injury causes glomerular damage remains elusive.

Wnt/β-catenin is a key signaling cascade that is critical for normal organogenesis. In this pathway, extracellular Wnts bind to cell-surface Frizzled receptors, transducing a signal that allows for the accumulation of cytoplasmic β-catenin, which then translocates to the nucleus and

regulates target genes (6). While highly active during development, Wnt/β-catenin signaling becomes quiescent in adult kidneys and reactivated during kidney injury (7-10). Activation of this signaling leads to a fibrotic response and promotes the progression of CKD via the upregulation of profibrotic mediators such as fibronectin, the renin-angiotensin system, plasminogen activator inhibitor-1 and matrix metalloproteinase-7 (MMP-7) (6, 11-13). Induction of MMP-7 by Wnt/β-catenin is particularly interesting, because it is the most robust β-catenin downstream target, and its expression primarily occurs in renal tubules (14-16). As a secreted protein that can be detected in the urine, MMP-7 is an effective noninvasive urinary biomarker for activation of Wnt/β-catenin after kidney injury (16, 17).

In the current study, we evaluated kidney injury after chronic infusion of angiotensin II (Ang II) using conditional knockout mice with tubule-specific ablation of β-catenin (18). Interestingly, although the genetic mutation was restricted to renal tubules, we found that these mice had significant protection against glomerular injury and proteinuria, accompanied by a reduced MMP-7 expression. These results were replicated in an adriamycin-induced proteinuria model. We further demonstrate that MMP-7 could degrade the slit diaphragm protein nephrin and impaired integrity of the glomerular filtration barrier. *In vivo* exposure of mice to elevated MMP-7 levels was sufficient to cause proteinuria, and global ablation of MMP-7 protected mice from Ang II-induced glomerular injury. Our findings illustrate that tubular injury promotes glomerular damage by β-catenin-driven release of MMP-7.

RESULTS

Mice with tubule-specific ablation of β-catenin are protected from Ang II-induced albuminuria and glomerular injury

Tubule-specific β-catenin knockout mice (Ksp-β-cat-/-), in which the β-catenin gene was specifically disrupted in renal tubular epithelia by mating the β-catenin-floxed mice and Ksp-cadherin promoter-driven Cre recombinase transgenic mice, were described and characterized previously (18). We exposed these mice to 1.5 mg/kg/day Ang II via osmotic minipumps, which causes significant glomerular injury and albuminuria (19-22). In contrast to age-, sex-matched, β-catenin-floxed littermates (Ksp-β-cat+/+), Ksp-β-cat-/- mice were significantly protected from albuminuria at 14, 21 and 28 days after chronic Ang II infusion (Figure 1A). Gel electrophoresis of mouse urine samples confirmed that the majority of the protein in the urine was in fact albumin (Figure 1B). Immunohistochemical staining for megalin and cubulin did not reveal any qualitative differences between Ang II-treated Ksp-β-cat+/+ and Ksp-β-cat-/- mice (Figure 1C), suggesting it was unlikely that a defect in tubular reabsorption of albumin was the cause for the increase in urinary albumin excretion.

We then investigated differences in glomerular injury between Ksp-β-cat+/+ and Ksp-β-cat-/- mice. At baseline there were no histologic differences between kidneys of naïve Ksp-β-cat+/+ mice and Ksp-β-cat-/- littermates (data not shown). However, kidneys from Ang II-treated Ksp-β-cat+/+ mice demonstrated increased glomerular injury, with focal areas of collapse and significant proteinuria in Bowman's space. In contrast, treated Ksp-β-cat-/- mice were protected from injury (Figure 1D). We further assessed expression of nephrin and Wilms tumor 1 (WT1). Nephrin is a key component of the glomerular slit diaphragm and plays an important role in preventing urinary albumin excretion (23). WT1 is a transcription factor important for

maintenance of normal podocyte differentiation (24). Control glomeruli at basal conditions demonstrated uninterrupted linear nephrin staining and abundant $WT1^+$ nuclei. Significant disruptions in nephrin distribution and fewer $WT1^+$ nuclei were observed in Ang II-treated Ksp-β-cat+/+ mice. The Ksp-β-cat-/- mice were partially protected from these Ang II effects (Figure 1, D-F). Immunoblotting analyses of kidney lysates confirmed the reduction of WT1 in Ksp-β-cat+/+ mice compared to Ksp-β-cat-/- littermates (Figure 1G).

Glomerular changes were also demonstrated on an ultrastructural level. Using transmission electron microscopy (TEM), we noted significant podocyte foot process effacement in the Ksp-β-cat+/+ mice compared to untreated controls (Figure 2, A and B). The Ksp-β-cat-/- mice were largely protected from foot process effacement (Figure 2C). Similar changes were noted on scanning electron microscopy (SEM) (Figure 2, D-F). These data demonstrate that Ksp-β-cat-/- mice are protected from podocyte injury, in spite of the fact that the genetic deletion is limited to the renal tubules.

Tubule-specific ablation of β-catenin protects mice from renal fibrosis induced by Ang II infusion

We compared the late fibrotic response to Ang II between Ksp-β-cat+/+ and Ksp-β-cat-/- mice. We found that Ksp-β-cat+/+ mice possessed significantly more fibrosis than Ksp-β-cat-/- mice at time of sacrifice (Figure 3A). Fibronectin protein levels tended to be higher in the Ksp-β-cat+/+ mice as well (Figure 3, B and C). Finally, serum creatinine levels were only increased when comparing Ang II-treated Ksp-β-cat+/+ mice to untreated controls. The Ksp-β-cat-/- mice creatinine values were not significantly different from either of the other groups (Figure 3D). This

indicates that not only are Ksp-β-cat-/- mice protected from glomerular injury, they are protected from chronic interstitial fibrosis and loss of renal function at late stages of disease.

Tubule-specific ablation of β-catenin inhibits renal MMP-7 expression

To determine the mechanism for why Ksp-β-cat-/- mice suffer less podocyte injury after Ang II exposure, we examined the levels of MMP-7, a secreted, low molecular weight metalloprotease that is a known direct target of β-catenin signaling (14). MMP-7 is not detectable by immunoblotting in normal kidneys (14). After Ang II treatment, MMP-7 levels were increased in Ksp-β-cat+/+, but not Ksp-β-cat-/-, kidneys (Figure 4, A and B). *MMP-7* gene expression showed a threefold higher mean in Ksp-β-cat+/+ and Ksp-β-cat-/- mice, although this did not reach significance (Figure 4C, P=0.092, n=5). MMP-7 protein was localized to renal tubules using immunohistochemistry and again showed greater expression in Ksp-β-cat+/+ compared to Ksp-β-cat-/- mice or untreated controls (Figure 4D). Based on these results, we hypothesized that MMP-7 plays a role in glomerular injury after chronic Ang II infusion.

Tubule-specific ablation of β-catenin protects against adriamycin-induced proteinuria and MMP-7 upregulation

In addition to the Ang II model above, we assessed wild type and Ksp-β-cat-/- mice after exposure to adriamycin, a well-known inducer of proteinuria. We found that Ksp-β-cat-/- mice had significantly less urinary albumin excretion than Ksp-β-cat+/+ mice (Figure 5, A and B). Nephrin levels were decreased in KSP-β-cat+/+ mice compared to KSP-β-cat-/- mice (Figure 5C). Further, Ksp-β-cat-/- mice expressed less MMP-7 by immunoblot and immunofluorescence

(Figure 5, D and E). This demonstrates that the effect of tubular β-catenin on MMP-7 expression and urinary albumin excretion is generalizable among proteinuric CKD states.

MMP-7 increases glomerular permeability *ex vivo* and depletes nephrin in glomerular cultures

To provide direct evidence for MMP-7 in mediating glomerular injury, we used an *ex vivo* glomerular culture model system. To this end, glomeruli were isolated from normal rat kidneys by a sieving method, and then exposed to recombinant MMP-7 protein (50 nM). As shown in Figure 6A, MMP-7 treatment clearly increased glomerular permeability *ex vivo*, leading to an increased release of albumin from glomerular capillary to surrounding media, in a glomerular permeability assay. This suggests that MMP-7 can impair the integrity of the glomerular filtration barrier. Electron microscopy confirmed that podocyte foot processes became effaced upon addition of MMP-7 to the culture medium (Figure 6B).

We further examined the effect of MMP-7 on the key slit diaphragm protein, nephrin, in cultured glomeruli *ex vivo*. As shown in Figure 6C, MMP-7 treatment rapidly decreased nephrin protein in cultured glomeruli, as nephrin abundance decreased after incubation with MMP-7 for 30 minutes. The action of MMP-7 on glomerular nephrin depletion was dose-dependent (Figure 6D). We found that nephrin depletion was dependent on the proteolytic activity of MMP-7, as use of an MMP-7 inhibitor (MMP Inhibitor II) blocked the effect (Figure 6E). Another MMP inhibitor that has no specific activity against MMP-7, GM6001, had no effect on nephrin depletion. These results indicate that MMP-7 can increase glomerular permeability and impair glomerular filtration integrity by degrading and depleting nephrin.

MMP-7 degrades nephrin via proteolytic cleavage

To determine the specificity of the MMP-7 effects on nephrin, isolated rat glomeruli were exposed to different MMPs including MMP-7, MMP-2 and MMP-9. As shown in Figure 7A, while MMP-7 caused nephrin depletion, both MMP-2 and MMP-9 did not, suggesting the specificity of MMP-7 action. We found that only MMP-7, but not the other MMPs, could also deplete podocin, another key component of the slit diaphragm (Figure 7B). Finally, all MMPs tested including MMP-2, MMP-7 and MMP-9 did not affect other plasma membrane proteins in podocytes such as integrin α3 and integrin β1, suggesting that MMP-7 had a specific effect on slit diaphragm proteins (Figure 7C).

To further examine the effects of MMP-7 on nephrin depletion, we utilized human embryonic kidney cells (HEK-293) transfected with nephrin expression vector and then incubated with recombinant MMP-7 (50 nM). Nephrin was depleted from HEK-293 cells in a time- and dose-dependent manner (Figure 8, A and B). Degradation also occurred when nephrin was immunoprecipitated from cell lysates and subsequently exposed to MMP-7, and this was blocked effectively by MMP inhibitor II (Figure 8C), demonstrating that MMP-7 is able to degrade nephrin protein in a cell-free system. To better confirm nephrin degradation by MMP-7, we incubated a truncated form of purified recombinant mouse nephrin protein with MMP-7 (Figure 8D). This truncated form of MMP-7 is 150 kDa in size and contains the majority of the extracellular domains of nephrin (corresponding to Gln37~Thr1049), but lacks the transmembrane segment and cytoplasmic tail (Figure 8E). After incubation with MMP-7, smaller proteolytic fragments of nephrin were detectable in SDS-PAGE (Figure 8D, arrows), which was accompanied by the reduction of 150 kDa truncated nephrin. These experiments indicate that MMP-7 is capable of

directly cleaving the nephrin protein, which would lead to slit diaphragm disruption, podocyte injury, and proteinuria.

Exposure to exogenous MMP-7 in vivo induces proteinuria

To provide direct evidence for MMP-7 in mediating podocyte injury *in vivo*, we examined the effect of MMP-7 overexpression on the integrity of the glomerular filtration barrier in healthy animals. To this end, an MMP-7 expression vector (pCMV-MMP-7) or empty vector (pcDNA3) were injected into normal wild-type mice using a hydrodynamic-based gene transfer approach via tail vein, which leads to transient expression of the transgene (25). We found that plasmid delivery led to upregulation of MMP-7 mRNA in both the liver and the kidney, although the hepatic expression was much higher (Supplemental Figure 1, A and B). MMP-7 protein could be detected at high levels circulating in the serum (Supplemental Figure 1C). With a molecular weight of 29kD we expect that it is freely filtered at the glomerulus to gain access to the slit diaphragm. As shown in Figure 9A, MMP-7 expression led to a significant increase in albuminuria. In a similar fashion, injection of recombinant MMP-7 protein (1 mg/kg) in mice also resulted in an increase in albuminuria, compared to vehicle controls (Figure 9B). These data suggest that elevated MMP-7 is sufficient to induce podocyte injury and impair glomerular filtration.

MMP-7 deficiency protects mice against proteinuria after Ang II infusion

To confirm the role of MMP-7 in mediating podocyte injury after Ang II infusion, we chronically infused Ang II *via* osmotic minipumps to wild-type (MMP-7+/+) and MMP-7 null mice (MMP-7-/-) to assess their response to proteinuric injury. As shown in Figure 10A, mice with global ablation of MMP-7 were significantly protected from albuminuria, compared to wild-

type controls. These results were further confirmed by gel electrophoresis (Figure 10B). Glomerular nephrin staining was significantly disrupted in wild-type kidneys compared to the MMP-7-/- mice (Figure 10C). MMP-7-/- mice were also protected from WT1 depletion by both immunostaining (Figure 10, C and D) and immunoblotting (Figure 10, E and F). Collectively, these data demonstrate that MMP-7 contributes to glomerular/podocyte injury and proteinuria after Ang II infusion.

DISCUSSION

Treatments for CKD remain extremely limited in scope and efficacy. Since 1993, angiotensin receptor blockers and angiotensin converting enzyme inhibitors have been the cornerstone of proteinuric CKD treatment, but these agents are only partially effective in reducing proteinuria, and often with significant unwanted side effects (26). This problem calls for better understanding of the exact cellular events leading to progressive CKD with proteinuria. Although it is intuitive to speculate that tubular injury would eventually influence glomerular integrity and health, the underlying mechanism connecting these two events was poorly understood.

The results presented in this study demonstrate that tubule-derived MMP-7 could have a profound effect on podocyte biology and glomerular filtration integrity. In mice with tubule-specific ablation of β-catenin, glomerular integrity is largely preserved after chronic infusion of Ang II. These effects are associated with reduced tubular expression of MMP-7, a robust and direct target of Wnt/β-catenin (14). MMP-7 directly degrades the key slit diaphragm protein nephrin, as well as podocin, and leads to impairment of glomerular filtration. Therefore, our studies provide evidence for the notion that MMP-7 mediates tubulo-glomerular communication in diseased kidneys. Previous studies have shown that there is a complex crosstalk between renal tubular cells and interstitial fibroblasts leading to the development of fibrosis (27-29). It has also been appreciated that primary glomerular injuries can lead to tubular injury, which is evidenced by the development of tubular atrophy and interstitial fibrosis in a variety of primary glomerular disorders (3). We now propose that the opposite can occur, in which tubule-derived mediators lead to an enhancement of glomerular injury. Tubular-to-glomerular crosstalk should not be surprising, considering the close apposition of renal tubules to glomeruli and the major role of the macula densa in regulating glomerular hemodynamics via nitric oxide and adenosine (30).

However, our results are unique in that a tubule-derived *protease* causes glomerular injury by direct degradation of the key slit diaphragm proteins in podocytes.

The means by which a soluble protease reaches the glomerulus requires further study, but could theoretically occur through several pathways including diffusion from nearby tubules. Further, it is well known that tubular injury can lead to tubular apoptosis, loss of barrier integrity and the potential back-leak of substances through injured tubules, which could affect glomeruli (31-34). Finally, it is possible that MMP-7 gains access to the systemic circulation. At 29 kDa, we would expect that some amount of MMP-7 could be freely filtered at the glomerulus to gain access to the slit diaphragm. These potential mechanisms require further exploration.

MMP-7 is a matrix metalloprotease that is highly upregulated in renal tubules during kidney injury. MMP-7 is increased in experimental unilateral ureteral obstruction, acute kidney injury, polycystic kidney disease, and adriamycin nephropathy, as well as in human kidney biopsies obtained from various CKD patients and in human urine after injury (14, 15, 35). It is a known target for β-catenin and its promoter contains two binding sites for the β-catenin transcription co-factor T cell factor (TCF). MMP-7 is associated with and stimulated by canonical Wnt signaling or β-catenin and can be blocked by Wnt or β-catenin inhibition (14). Our studies using Ang II infusion (Figure 4) and adriamycin (Figure 5) demonstrate that tubule-specific β-catenin knockout mice have reduced MMP-7 expression after injury, in agreement with prior studies using other experimental kidney injuries (36). The induction of MMP-7 in a wide variety of CKD models is consistent with the notion that glomerular injury and proteinuria are an inevitable consequence of perhaps all CKD, regardless of the initial etiologies.

Besides matrix proteins, the substrates of MMP-7 include several extracellular, non-matrix proteins, such as E-cadherin, Fas ligand, defensins, and other MMPs (14, 36, 37). For the first

time, we now demonstrate that nephrin is a specific and direct substrate of MMP-7. This conclusion is supported by several lines of evidence. First, MMP-7 can degrade nephrin in cultured glomeruli, cultured cells and cell-free system, which is dependent on its proteolytic activity. Second, the action of MMP-7 on nephrin degradation is rapid, starting as early as 5 minutes after incubation (Figure 6). Third, the action of MMP-7 on nephrin is direct, cleaving purified recombinant nephrin protein in a cell-free system (Figure 8). Finally, the action of MMP-7 is specific, as other MMPs such as MMP-2 and MMP-9 are unable to degrade nephrin in the same conditions. Notably, MMP-7 also decreases levels of podocin in cultured glomeruli (Figure 7), suggesting it cleaves podocin as well, although it has no effect on other podocyte membrane proteins including integrin α3 and integrin β1. However, we cannot exclude the possibility that decrease of podocin in cultured glomeruli after MMP-7 incubation could be a result of nephrin loss, because nephrin/podocin often form complexes and stabilize each other. Regardless of the mechanism involved, the loss of key slit diaphragm proteins such as nephrin and podocin would be sufficient, by themselves, to increase glomerular permeability and impair glomerular filtration (38). Consistent with this view, exogenous MMP-7 is sufficient to induce proteinuria in mice (Figure 9). Although the effects of injected MMP-7 are transient in mouse model, we would anticipate that, in CKD settings, MMP-7 is produced chronically and continuously and therefore would lead to detrimental effects on the integrity of glomerular filtration (15).

MMP-7 null mice are also protected against proteinuric kidney disease (Figure 10). We must acknowledge that mice with global deficiency of MMP-7 cannot definitively prove the involvement of tubular MMP-7 in glomerular disease, and tubular-specific MMP-7 null mice unfortunately do not exist. Nevertheless, the work with MMP-7 null mice provide further support of the importance of this protease in proteinuria.

It should be pointed out that Ksp-β-cat-/- mice are also protected from the Ang II-induced development of interstitial fibrosis (Figure 3). This is not surprising, as earlier studies have shown that β-catenin-driven MMP-7 is a pathogenic mediator of kidney fibrosis by degrading E-cadherin, which leads to β-catenin liberation and activation, forming a vicious cycle (16). Furthermore, this reduction of fibrosis in Ksp-β-cat-/- mice after Ang II infusion could be a result of the diminished glomerular injury and proteinuria, because proteinuria, *per se*, aggravates tubulointerstitial lesions as described previously (39, 40). In addition, the activation of tubular β-catenin after Ang II infusion could have a number of MMP-7-independent effects that promote interstitial fibrosis, including effects on the expression of the renin-angiotensin system, Snail1, and fibronectin (6, 7, 41). Therefore, tubular β-catenin signaling during AngII exposure could, through multiple pathways, lead to progressive interstitial fibrosis that is characteristic of all forms of CKD.

Overall, these studies uncover a novel mechanism to account for how tubular injury triggers glomerular damage during CKD progression. We show that kidney injuries after Ang II infusion or adriamycin exposure lead to tubular β-catenin activation, which in turn upregulates soluble MMP-7 expression in renal tubules. Such tubule-derived MMP-7 causes deleterious glomerular changes including the cleavage of nephrin and result in glomerular filtration impairment and higher urinary protein excretion. This would lead to further tubular β-catenin activation and MMP-7 expression in a positive feedback loop that ultimately contributes to progressive renal failure and fibrosis. Therapies directed against β-catenin and MMP-7 could be useful in the treatment of CKD.

METHODS

Animals and treatment protocol

Tubule-specific β-catenin knockout mice (Ksp-β-cat-/-) were generated as previously described and are on the C57BL/6 background strain (18). Ksp-β-cat+/+ controls were β-catenin-floxed, Cre-negative littermates. Mice were 8-10 weeks at initiation of the experiments, and age and sex were equally distributed in both groups. MMP-7-/- (null) mice and wild type C57BL/6J mice were obtained from The Jackson Laboratory (Stock 005111 and 000664; Bar Harbor, ME).

To sensitize mice to the Ang II model, a unilateral nephrectomy was performed on day -7. On day 0, an osmotic minipump (Alzet, Cupertino CA) was implanted subcutaneously. The minipump delivered 1.5 mg/kg/day of Ang II (Bachem, Torrance CA) as previously described (19). Urine was collected weekly until sacrifice, at which time the kidneys, serum, and final urine sample were collected. Adriamycin injury was induced with a single intravenous dose of 22 mg/kg in non-nephrectomized mice. This high dose of adriamycin is necessary to induce injury in the resistant C57BL/6 strain and was titrated empirically prior to our experiment (42, 43).

Histology

For histologic assessment, kidneys were fixed in 10% buffered formalin, embedded in paraffin, and cut at 3 μm thick sections for analysis. Masson's trichrome staining was performed with a kit from Thermo Fisher Scientific (Waltham, MA).

Renal function measurements

Serum creatinine was determined with an assay kit (catalog #C7548, Pointe Scientific, Canton MI) using an enzymatic method that is superior to Jaffe assays and compares favorably with HPLC

methods (44). Urinary albumin excretion (albuminuria) was detected by use of a mouse albumin ELISA kit (Bethyl Laboratories, Worthington, TX). Urinary albumin was normalized to the urine creatinine which was determined using the same creatinine kit noted above. Urine samples were loaded by equivalent urinary creatinine levels into polyacrylamide gels and subjected to electrophoresis prior to staining with Coomassie blue.

Immunofluorescence

Frozen kidney samples were embedded at sacrifice in OCT medium (Scigen Scientific, Gardena, CA) and sections cut on a microtome at 3 μm thickness. Sections were then fixed in 4% paraformaldehyde, followed by permeabilization in 0.2% Triton in PBS. Sections were blocked with normal serum then incubated overnight in primary antibody for nephrin (#2OR-NP002; Fitzgerald Industries, Acton MA) and WT1 (#sc-192; Santa Cruz Biotechnology, Santa Cruz, CA). FITC- and Cy3-conjugated secondary antibodies (Jackson ImmunoResearch Laboratories, West Grove, PA) were used for detection. Sections were visualized on a Leica SP5 CW-STED confocal microscope.

To determine the percentage of glomeruli with disrupted nephrin, at least 20 glomeruli for each animal were evaluated. Any breaks in the normal linear nephrin staining were counted as positive for disruption. For WT1-positive cells, at least 20 glomeruli were evaluated for each animal. The number of WT1-positive cells per glomerulus were counted and averaged per animal, and these numbers were averaged for a group mean.

Immunohistochemistry

Three micron paraffin embedded sections were deparaffinized and rehydrated through graded ethanol (100%, 95% and 70%) to distilled water and subjected to antigen retrieval with 10 mM sodium citrate (pH 6.0) buffer for 30 minutes. Sections were then incubated with 3% H_2O_2 to block endogenous peroxidase activity, permeabilized in PBS-Tween (PBS-T) and blocked in 3% bovine serum albumin (BSA) before incubating overnight with anti-cubulin (sc-25470), anti-megalin (sc-20609, both from Santa Cruz Biotechnology), and anti-MMP-7 antibodies (#GTX11716, Genetex, Irvine CA). Immunohistochemical staining was performed according to the established protocol as described previously (19).

Immunoblotting

Kidneys were homogenized in RIPA buffer containing a protease inhibitor cocktail (#78442, Thermo Fisher) and concentration determined with BCA protein assay (Thermo Fisher). Gel electrophoresis was performed on reduced, denatured samples. After blotting onto PVDF membranes (GE Healthcare Lifesciences, Pittsburgh PA) and blocking with 5% milk, membranes were incubated with primary antibodies. HRP-conjugated secondary antibodies and Supersignal West Pico substrate (Thermo Fisher) were used for detection. Densitometry was performed using Image J software (NIH, Bethesda, MD). The following primary antibodies were used: MMP-7 (#GTX11716, Genetex), fibronectin (#F3648, Millipore Sigma), actin (#MAB1501, Millipore Sigma), WT1 (#sc-192, Santa Cruz Biotechnology), integrin-α3 and integrin β1 (#611044 and 610468, BD Biosciences, San Jose CA).

Quantitative, real-time reverse transcriptase PCR (qRT-PCR)

RNA was isolated from kidney tissue homogenates using TRIzol reagent (Thermo Fisher). A reverse transcriptase reaction was performed to obtain cDNA, and this was utilized in a qRT-PCR reaction using SYBR green in a CFX Connect instrument (BioRad, Hercules CA). The primer sequences to detect mouse *MMP-7* are 5'-TAGGCGGAGATGCTCACTTT-3' (FWD), and 5'-TTCTGAATGCCTGCAATGTC-3' (REV), while human *MMP-7* (for detection of plasmid derived MMP-7) was detected with 5'- TTGATGGGCCAGGAAACACG-3' (FWD) and 5'-CTACCATCCGTCCAGCGTTC-3' (REV). Melt curves were utilized to ensure the specificity of the PCR product. Data were analyzed using the $2^{-\Delta\Delta Ct}$ method (45).

MMP-7 ELISA

An ELISA for human total MMP-7 was performed on serum samples from mice injected with human MMP-7 plasmid following instructions from the manufacturer (R&D Systems, cat# DMP700, Minneapolis, MN).

***Ex vivo* glomerular cultures**

To obtain primary rat glomeruli for culture, adult male Sprague Dawley rats (Envigo, Indianapolis, IN) were anesthetized and their kidneys were removed. Each kidney was carefully minced and passed through three sequentially smaller sieves to remove renal tubules and allow glomeruli to pass through per previously described protocol (46). The flow-through was centrifuged to pellet the glomeruli, and this was resuspended in RPMI-1640 with 10% FBS and 100U/ml penicillin/streptomycin. MMP-2, MMP-7, and MMP-9 (R&D Systems, Minneapolis MN) and GM6001 and MMP Inhibitor II (both from EMD Millipore, Billerica MA) were added as described.

To determine albumin permeability, we performed experiments as previously described (47). Briefly, *ex vivo* glomeruli were incubated in media containing 5% bovine serum albumin (BSA, Sigma Aldrich, St. Louis MO). Recombinant MMP-7 was then added and incubated for 30 minutes. Glomeruli were then washed and incubated in low BSA media and samples collected at 30 minutes and 1 hour. The BSA content of this media was determined by ELISA (Bethyl Laboratories).

MMP-7 plasmid

An active mutant human MMP-7 clone with a substitution of valine to glycine at amino acid 92 was kindly provided by Dr. Carole L. Wilson (Medical University of South Carolina, Charleston, SC). The full-length coding sequence of MMP-7 cDNA was amplified by using a standard RT-PCR protocol. The PCR product was cloned into the mammalian expression vector p3XFlag-CMV (Sigma Aldrich) and confirmed by DNA sequencing at the University of Pittsburgh Biomedical Research Support Facilities. Plasmid was injected into mice via tail vein at a dose of 2 mg/kg plasmid in a 2 mL volume delivered within a 10-second time period, as adapted from prior published protocols (25).

Transmission Electron Microscopy (TEM)

TEM and scanning electron microscopy (SEM) were performed as previously described (48). Portions of mouse kidneys were immersion-fixed with 2.5% glutaraldehyde in PBS for more than 24 hours. Several 1 mm^3 cubes were obtained, washed 3x in PBS then post-fixed in aqueous 1% OsO_4, 1% $K_3Fe(CN)_6$ for 1 hour. Following 3 PBS washes, the pellet was dehydrated through a graded series of 30-100% ethanol, 100% propylene oxide then infiltrated in 1:1 mixture of

propylene oxide:Polybed 812 epoxy resin (Polysciences, Warrington, PA) for 1 hr. After several changes of 100% resin over 24 hours, the pellet was embedded in molds, cured at 37ºC overnight, followed by additional hardening at 65ºC for two more days. Ultrathin (60 nm) sections were cut on a Leica EM UC7 ultramicrotome, collected on 200 mesh copper grids, stained with 4% uranyl acetate for 10 minutes, followed by 1% lead citrate for 7 min using the Leica EM AC20 automatic stainer. Sections were imaged using a JEOL JEM 1011 transmission electron microscope (Peabody, MA) at 80 kV fitted with a side mount AMT 2k digital camera (Advanced Microscopy Techniques, Danvers, MA).

Scanning Electron Microscopy (SEM)

Kidney tissue was processed as for TEM above, but 1 mm thick longitudinal slices were used instead of cubes. Tissue was processed up to the final 100% ethanol, and then chemically dried using hexamethyldisilazane. Dried slices were mounted onto aluminum stubs, grounded with silver paint and then sputter coated with 3.5 nm gold/palladium (Auto 108, Cressington, Watford, UK). Samples were viewed in a JEOL JSM-6330F scanning electron microscope (Peabody, MA) at 3 kV.

Statistics

Data are presented as mean ± SEM. A student's t-test (two-tailed) was used for comparisons between two groups, while a one-way ANOVA was utilized for more than two groups. $P < 0.05$ was the threshold used for significance. Statistical tests were run on GraphPad Prism (San Diego, CA).

Animal study approval

All studies using animals were performed to the ethical and scientific standards recommended by the Guide for the Care and Use of Laboratory Animals of the NIH. The animal protocol was approved by the Institutional Animal Care and Use Committee at the University of Pittsburgh.

AUTHOR CONTRIBUTIONS

RJT, YLi, BMR, DMC, DZ, JH, DBS, and YLiu designed the experiments. RJT, YLi, BMR, DMC, and DZ performed the experiments. RJT, YLi, BMR, DMC, DZ, DBS, and YLiu analyzed the results. RJT and YLiu wrote the manuscript. All authors reviewed the final version of the manuscript.

ACKNOWLEDGMENTS

This work was supported by funding from NIH grants R01DK064005 and R01DK106049 (to YLiu), R01DK103776 (JH), P30DK079307 (Pittsburgh Center for Kidney Research), and National Science Foundation of China grant 81521003. RJT was supported by NIH T32DK061296, an American Heart Association Award 13FTF160990086, an American Society of Nephrology Carl W. Gottschalk Research Scholarship Grant, a University of Pittsburgh Medical Center Competitive Medical Research Fund, and a University of Pittsburgh Physicians Academic Foundation Award. DMC was supported by a Nephrotic Syndrome Study Network Career Development Fellowship. DZ is supported by NIH K01DK116816.

FIGURE LEGENDS

Figure 1. Tubule-specific β-catenin knockout mice are protected from glomerular injury. The β-cat-floxed mice (Ksp-β-cat+/+) and tubule-specific β-catenin knockouts (Ksp-β-cat-/-) were subjected to continuous angiotensin II (Ang II) infusions (1.5 mg/kg/day, osmotic minipump). (A) Urinary albumin excretion was measured in the Ksp-β-cat+/+ and Ksp-β-cat-/- mice (n=6) at 14, 21, and 28 days after Ang II infusion. * $P < 0.05$ compared to Ksp-β-cat+/+ at same timepoint, one-way ANOVA. (B) Gel electrophoresis of urine samples shows the composition of the protein excreted in the urine. Albumin is indicated. Urine from an untreated control mouse (Ctrl, lane 1) was included for reference. (C) Levels of megalin and cubulin are not different between Ksp-β-cat+/+ and Ksp-β-cat-/- mice after Ang II infusion. (D) Evaluation of glomerular histology reveals increased glomerular damage in the Ksp-β-cat+/+ compared to Ksp-β-cat-/- mice. Note the high levels of protein in Bowman's space in the Ksp-β-cat+/+ (asterisk), accompanied by significant glomerulosclerosis (arrow). In the Ksp-β-cat-/- mice overall glomerular injury including glomerulosclerosis was minimal. A control (Ctrl, untreated mouse) glomerulus is provided for reference. Immunofluorescence revealed significant disruption in nephrin and fewer WT1-positive podocytes in the Ksp-β-cat+/+ compared Ksp-β-cat-/- mice. (E) Quantitation of number of glomeruli with abnormal nephrin staining and (F) WT1-positive nuclei per glomeruli (n=5, *$P < 0.05$, one way ANOVA). (G) Immunoblot for WT1 showing depleted levels in the Ksp-β-cat+/+ mice, compared to Ksp-β-cat-/- mice. *$P < 0.05$, t-test.

Figure 2. Podocyte foot process integrity is preserved in Ksp-β-cat-/- mice after Ang II infusion. Mice were treated as in Figure 1. (A-C) Transmission electron microscopy (TEM) showing extensive foot process effacement (arrows) in Ang II-treated Ksp-β-cat+/+ mice

compared to Ksp-β-cat-/- mice. Bar equals 500 nm. (D-F) Scanning electron microscopy (SEM) revealed significant effacement in the control mice compared to untreated control and Ang II-treated Ksp-β-cat-/- mice. Bar equals 5 μm.

Figure 3. Ablation of β-catenin in renal tubules reduces interstitial fibrosis induced by Ang II infusion. (A) Masson's trichrome staining showing increased fibrosis in Ksp-β-cat+/+ mice after Ang II infusion (asterisk), compared to Ksp-β-cat-/- mice. (B) Western blots show a trend towards increased levels of fibronectin in the control mice, compared to Ksp-β-cat-/- mice (n=4). $P = 0.06$, t-test. (C) Measurement of serum creatinine shows that the only significant difference is observed between untreated control mice (Ctrl) and Ksp-β-cat+/+ mice, suggesting moderation of injury in the Ksp-β-cat-/- mice (n=5). * $P < 0.05$, one-way ANOVA.

Figure 4. Renal expression of MMP-7 is reduced in Ksp-β-cat-/- mice after Ang II infusion. **(**A, B) Western blot analyses for MMP-7 reveal significant reduction in the Ksp-β-cat-/- mice after Ang II infusion, compared to Ksp-β-cat+/+ mice (n=4). Western blot (A) and quantitation after densitometry (B) are shown. *$P < 0.05$, t-test. (C) qRT-PCR shows a trend to higher expression of MMP-7 mRNA in the Ksp-β-cat+/+ mice as well (n=5, t-test). $P = 0.092$ two tailed, 0.046 one tailed. (D) Immunohistochemical staining for MMP-7 shows negligible staining in control mice, with dramatic upregulation in Ang II-treated Ksp-β-cat+/+ mice (arrows). A reduced MMP-7 staining was noticed in Ksp-β-cat-/- mice. Bar equals 50μM.

Figure 5. KSP-β-cat-/- mice are protected from adriamycin-induced kidney injury and proteinuria. (A) Urine albumin excretion 3 weeks after injection of adriamycin (22mg/kg) in

KSP-β-cat+/+ compared to KSP-β-cat-/- mice (* P < 0.05, t-test). (B) Gel electrophoresis of urine samples showing reduction in albumin excretion in KSP-β-cat-/- mice. (C) Immunofluorescence showing greater nephrin disruption in KSP-β-cat-/- mice. (D) Western blot demonstrating reduced kidney expression of MMP-7 in KSP-β-cat-/- mice. (D) Immunofluorescence for MMP-7 reveals strong upregulation in tubules from KSP-β-cat+/+ mice only.

Figure 6. Recombinant MMP-7 decreases nephrin in a time- and dose-dependent manner in *ex vivo* glomeruli. (A) MMP-7 treatment (50 nM, 30 min) causes a significant time-dependent release of albumin from isolated rat glomeruli. *$P < 0.05$, repeated measures one way ANOVA. (B) TEM of isolated glomeruli shows flattening and fusion of foot processes in MMP-7-treated glomeruli compared to vehicle controls (arrows). In separate experiments, glomeruli were incubated with either the same concentration of MMP-7 (50 nM) for various periods of time (C) or with increasing amounts of MMP-7 for 60 minutes (D). Glomerular lysates were immunoblotted with antibodies against nephrin and actin. (E) Nephrin depletion by MMP-7 is dependent on its proteolytic activity. Rat glomeruli were pretreated with GM6001 (25 μM) or MMP inhibitor II (20 μM) for 30 minutes before incubation with MMP-7 (25 nM or 50 nM) for 60 minutes.

Figure 7. MMP-7 reduces nephrin and podocin levels in isolated glomeruli. (A) Rat glomeruli were incubated separately with MMP-2 (1 μg/ml, or 13.88 nM), MMP-7 (50 nM) and MMP-9 (1 μg/ml, or 10.9nM) and total protein immunoblotted for nephrin. Only MMP-7 was capable of reducing nephrin levels. (B) MMP-7 also reduces podocin protein in isolated glomeruli *ex vivo*. Glomerular lysates were immunoblotted with antibodies against podocin and actin. (C) MMP-7

does not affect other membrane proteins in podocytes such as integrin-α3 and integrin-β1. Western blot analyses of glomerular lysates reveal no effect on integrin-α3 and -β1 proteins after incubation with any of the three MMPs.

Figure 8. MMP-7 mediates nephrin degradation *in vitro*. (A, B) HEK-293 cells were transfected with nephrin expression vector for 48 hours, followed by incubation with MMP-7 (50 nM) for various periods of time (A) or with increasing amounts of MMP-7 for 60 minutes (B). (C) Nephrin from overexpressing cells was immunoprecipitated with anti-nephrin antibody, followed by various treatments as indicated. MMP-7 caused nephrin depletion, which was inhibited by MMP inhibitor II. (D, E) Representative SDS-PAGE shows that MMP-7 degrades recombinant mouse nephrin protein. Purified mouse nephrin protein (2 μg) was incubated with 50 nM MMP-7 for 60 minutes. Truncated form of mouse nephrin corresponding to Gln37 to Thr1049 (~150 kDa in size) is used (E). Arrows in Panel (D) indicate the degradation fragments of nephrin.

Figure 9. Delivery of MMP-7 gene or recombinant MMP-7 protein induces albuminuria *in vivo.* (A) Mice were injected intravenously with pcDNA3 or pCMV-MMP-7 vector (2 mg/kg), respectively. Urinary albumin concentration was assayed 24 h after injection. $^{*}P < 0.05$ (n=7, t-test). (B) After injection with recombinant MMP-7 (1 mg/kg) for 3 hours, urinary albumin excretion was increased in the MMP-7-treated group, compared with vehicle controls. * $P < 0.05$ (n=6, t-test).

Figure 10. Mice with global ablation of MMP-7 are protected from Ang II-induced glomerular injury. Wild type (WT) and MMP-7-/- (KO) mice were treated with continuous

infusions of Ang II (1.5 mg/kg/day). (A) Albuminuria is significantly reduced in the KO compared to WT mice. (B) Gel electrophoresis of urine samples demonstrate a reduced albumin excretion in MMP-7-/- mice, compared to MMP-7+/+ counterparts. (C) Immunofluorescence staining shows extensive nephrin disruption and a decrease in numbers of healthy WT1-positive podocytes in MMP-7+/+ mice. MMP-7 KO mice retained linear nephrin staining and numbers of WT1-positive nuclei. (D) Quantitation of WT1-positive nuclei per glomerulus (n=5-6, t-test). (E, F) Western blot analyses show an increased preservation of WT1 expression in MMP-7-/- mice after Ang II infusion, compared to MMP-7+/+ controls. Western blot (E) and quantitation (F) are shown. *$P < 0.05$ (n=4-5, t-test).

Supplemental Figure 1. MMP-7 expression after plasmid injection. MMP-7 plasmid was injected via tail vein in wild type mice. After 18 hours, mice were euthanized and liver, kidney, and serum obtained. mRNA levels of MMP-7 were measured in the (A) liver and (B) kidney and circulating serum protein levels were assessed with an ELISA. (* $P < 0.05$, t-test).

REFERENCES

1. Centers for Disease Control and Prevention. Chronic Kidney Disease Surveillance System - United States. http://www.cdc.gov/ckd.
2. Abbate M, Zoja C, and Remuzzi G. How does proteinuria cause progressive renal damage? *J Am Soc Nephrol.* 2006;17(11):2974-84.
3. Kriz W, and LeHir M. Pathways to nephron loss starting from glomerular diseases-insights from animal models. *Kidney Int.* 2005;67(2):404-19.
4. Carlstrom M, Wilcox CS, and Arendshorst WJ. Renal autoregulation in health and disease. *Physiol Rev.* 2015;95(2):405-511.
5. Grgic I, Campanholle G, Bijol V, Wang C, Sabbisetti VS, Ichimura T, et al. Targeted proximal tubule injury triggers interstitial fibrosis and glomerulosclerosis. *Kidney Int.* 2012;82(2):172-83.
6. Tan RJ, Zhou D, Zhou L, and Liu Y. Wnt/beta-catenin signaling and kidney fibrosis. *Kidney Int Suppl (2011).* 2014;4(1):84-90.
7. DiRocco DP, Kobayashi A, Taketo MM, McMahon AP, and Humphreys BD. Wnt4/beta-catenin signaling in medullary kidney myofibroblasts. *J Am Soc Nephrol.* 2013;24(9):1399-412.
8. Kawakami T, Ren S, and Duffield JS. Wnt signalling in kidney diseases: dual roles in renal injury and repair. *J Pathol.* 2013;229(2):221-31.
9. Lin SL, Li B, Rao S, Yeo EJ, Hudson TE, Nowlin BT, et al. Macrophage Wnt7b is critical for kidney repair and regeneration. *Proc Natl Acad Sci U S A.* 2010;107(9):4194-9.
10. Edeling M, Ragi G, Huang S, Pavenstadt H, and Susztak K. Developmental signalling pathways in renal fibrosis: the roles of Notch, Wnt and Hedgehog. *Nat Rev Nephrol.* 2016;12(7):426-39.
11. Maarouf OH, Aravamudhan A, Rangarajan D, Kusaba T, Zhang V, Welborn J, et al. Paracrine Wnt1 Drives Interstitial Fibrosis without Inflammation by Tubulointerstitial Cross-Talk. *J Am Soc Nephrol.* 2015.
12. Xiao L, Zhou D, Tan RJ, Fu H, Zhou L, Hou FF, et al. Sustained Activation of Wnt/beta-Catenin Signaling Drives AKI to CKD Progression. *J Am Soc Nephrol.* 2015.

13. Zhou L, Li Y, Hao S, Zhou D, Tan RJ, Nie J, et al. Multiple genes of the renin-angiotensin system are novel targets of Wnt/beta-catenin signaling. *J Am Soc Nephrol.* 2015;26(1):107-20.
14. He W, Tan RJ, Li Y, Wang D, Nie J, Hou FF, et al. Matrix metalloproteinase-7 as a surrogate marker predicts renal Wnt/beta-catenin activity in CKD. *J Am Soc Nephrol.* 2012;23:294-304.
15. Surendran K, Simon TC, Liapis H, and McGuire JK. Matrilysin (MMP-7) expression in renal tubular damage: association with Wnt4. *Kidney Int.* 2004;65(6):2212-22.
16. Zhou D, Tian Y, Sun L, Zhou L, Xiao L, Tan RJ, et al. Matrix Metalloproteinase-7 Is a Urinary Biomarker and Pathogenic Mediator of Kidney Fibrosis. *J Am Soc Nephrol.* 2017;28(2):598-611.
17. Yang X, Chen C, Teng S, Fu X, Zha Y, Liu H, et al. Urinary Matrix Metalloproteinase-7 Predicts Severe AKI and Poor Outcomes after Cardiac Surgery. *J Am Soc Nephrol.* 2017;28(11):3373-82.
18. Zhou D, Li Y, Lin L, Zhou L, Igarashi P, and Liu Y. Tubule-specific ablation of endogenous beta-catenin aggravates acute kidney injury in mice. *Kidney Int.* 2012;82(5):537-47.
19. Tan RJ, Zhou D, Xiao L, Zhou L, Li Y, Bastacky SI, et al. Extracellular Superoxide Dismutase Protects against Proteinuric Kidney Disease. *J Am Soc Nephrol.* 2015;26(10):2447-59.
20. Zhou Y, Yu J, Liu J, Cao R, Su W, Li S, et al. Induction of cytochrome P450 4A14 contributes to angiotensin II-induced renal fibrosis in mice. *Biochim Biophys Acta Mol Basis Dis.* 2018;1864(3):860-70.
21. Eckel J, Lavin PJ, Finch EA, Mukerji N, Burch J, Gbadegesin R, et al. TRPC6 enhances angiotensin II-induced albuminuria. *J Am Soc Nephrol.* 2011;22(3):526-35.
22. Cechova S, Dong F, Chan F, Kelley MJ, Ruiz P, and Le TH. MYH9 E1841K Mutation Augments Proteinuria and Podocyte Injury and Migration. *J Am Soc Nephrol.* 2018;29(1):155-67.
23. Kandasamy Y, Smith R, Lumbers ER, and Rudd D. Nephrin - a biomarker of early glomerular injury. *Biomark Res.* 2014;2:21.
24. Zhou L, Li Y, He W, Zhou D, Tan RJ, Nie J, et al. Mutual Antagonism of Wilms' Tumor 1 and beta-Catenin Dictates Podocyte Health and Disease. *J Am Soc Nephrol.* 2014.

25. Liu F, Song Y, and Liu D. Hydrodynamics-based transfection in animals by systemic administration of plasmid DNA. *Gene Ther.* 1999;6(7):1258-66.

26. Johnson SA, and Spurney RF. Twenty years after ACEIs and ARBs: emerging treatment strategies for diabetic nephropathy. *Am J Physiol Renal Physiol.* 2015;309(10):F807-20.

27. Fabian SL, Penchev RR, St-Jacques B, Rao AN, Sipila P, West KA, et al. Hedgehog-Gli pathway activation during kidney fibrosis. *Am J Pathol.* 2012;180(4):1441-53.

28. Gewin L, Zent R, and Pozzi A. Progression of chronic kidney disease: too much cellular talk causes damage. *Kidney Int.* 2017;91(3):552-60.

29. Qi R, and Yang C. Renal tubular epithelial cells: the neglected mediator of tubulointerstitial fibrosis after injury. *Cell Death Dis.* 2018;9(11):1126.

30. Komlosi P, Bell PD, and Zhang ZR. Tubuloglomerular feedback mechanisms in nephron segments beyond the macula densa. *Curr Opin Nephrol Hypertens.* 2009;18(1):57-62.

31. Xiong C, Zang X, Zhou X, Liu L, Masucci MV, Tang J, et al. Pharmacological inhibition of Src kinase protects against acute kidney injury in a murine model of renal ischemia/reperfusion. *Oncotarget.* 2017;8(19):31238-53.

32. Wang S, Pan Q, Xu C, Li JJ, Tang HX, Zou T, et al. Massive Proteinuria-Induced Injury of Tubular Epithelial Cells in Nephrotic Syndrome is Not Exacerbated by Furosemide. *Cell Physiol Biochem.* 2018;45(4):1700-6.

33. Morais C, Westhuyzen J, Metharom P, and Healy H. High molecular weight plasma proteins induce apoptosis and Fas/FasL expression in human proximal tubular cells. *Nephrol Dial Transplant.* 2005;20(1):50-8.

34. Gao L, Liu MM, Zang HM, Ma QY, Yang Q, Jiang L, et al. Restoration of E-cadherin by PPBICA protects against cisplatin-induced acute kidney injury by attenuating inflammation and programmed cell death. *Lab Invest.* 2018;98(7):911-23.

35. Liang J, Lin G, Tian J, Chen J, Liang R, Chen Z, et al. Measurement of urinary matrix metalloproteinase-7 for early diagnosis of acute kidney injury based on an ultrasensitive

immunomagnetic microparticle-based time-resolved fluoroimmunoassay. *Clin Chim Acta.* 2019;490:55-62.

36. Zhou D, Tan RJ, Zhou L, Li Y, and Liu Y. Kidney tubular beta-catenin signaling controls interstitial fibroblast fate via epithelial-mesenchymal communication. *Sci Rep.* 2013;3:1878.

37. Tan RJ, and Liu Y. Matrix metalloproteinases in kidney homeostasis and diseases. *Am J Physiol Renal Physiol.* 2012;302(11):F1351-61.

38. Grahammer F, Schell C, and Huber TB. The podocyte slit diaphragm--from a thin grey line to a complex signalling hub. *Nat Rev Nephrol.* 2013;9(10):587-98.

39. Erkan E. Proteinuria and progression of glomerular diseases. *Pediatr Nephrol.* 2013;28(7):1049-58.

40. Gorriz JL, and Martinez-Castelao A. Proteinuria: detection and role in native renal disease progression. *Transplant Rev (Orlando).* 2012;26(1):3-13.

41. Hao S, He W, Li Y, Ding H, Hou Y, Nie J, et al. Targeted inhibition of beta-catenin/CBP signaling ameliorates renal interstitial fibrosis. *J Am Soc Nephrol.* 2011;22(9):1642-53.

42. Jeansson M, Bjorck K, Tenstad O, and Haraldsson B. Adriamycin alters glomerular endothelium to induce proteinuria. *J Am Soc Nephrol.* 2009;20(1):114-22.

43. Lee VW, and Harris DC. Adriamycin nephropathy: a model of focal segmental glomerulosclerosis. *Nephrology (Carlton).* 2011;16(1):30-8.

44. Keppler A, Gretz N, Schmidt R, Kloetzer HM, Groene HJ, Lelongt B, et al. Plasma creatinine determination in mice and rats: an enzymatic method compares favorably with a high-performance liquid chromatography assay. *Kidney Int.* 2007;71(1):74-8.

45. Schmittgen TD, and Livak KJ. Analyzing real-time PCR data by the comparative C(T) method. *Nat Protoc.* 2008;3(6):1101-8.

46. Rush BM, Small SA, Stolz DB, and Tan RJ. An Efficient Sieving Method to Isolate Intact Glomeruli from Adult Rat Kidney. *J Vis Exp.* 2018(141).

686 47. Vassiliadis J, Bracken C, Matthews D, O'Brien S, Schiavi S, and Wawersik S. Calcium mediates
687 glomerular filtration through calcineurin and mTORC2/Akt signaling. *J Am Soc Nephrol.*
688 2011;22(8):1453-61.
689 48. Wack KE, Ross MA, Zegarra V, Sysko LR, Watkins SC, and Stolz DB. Sinusoidal ultrastructure
690 evaluated during the revascularization of regenerating rat liver. *Hepatology.* 2001;33(2):363-78.
691

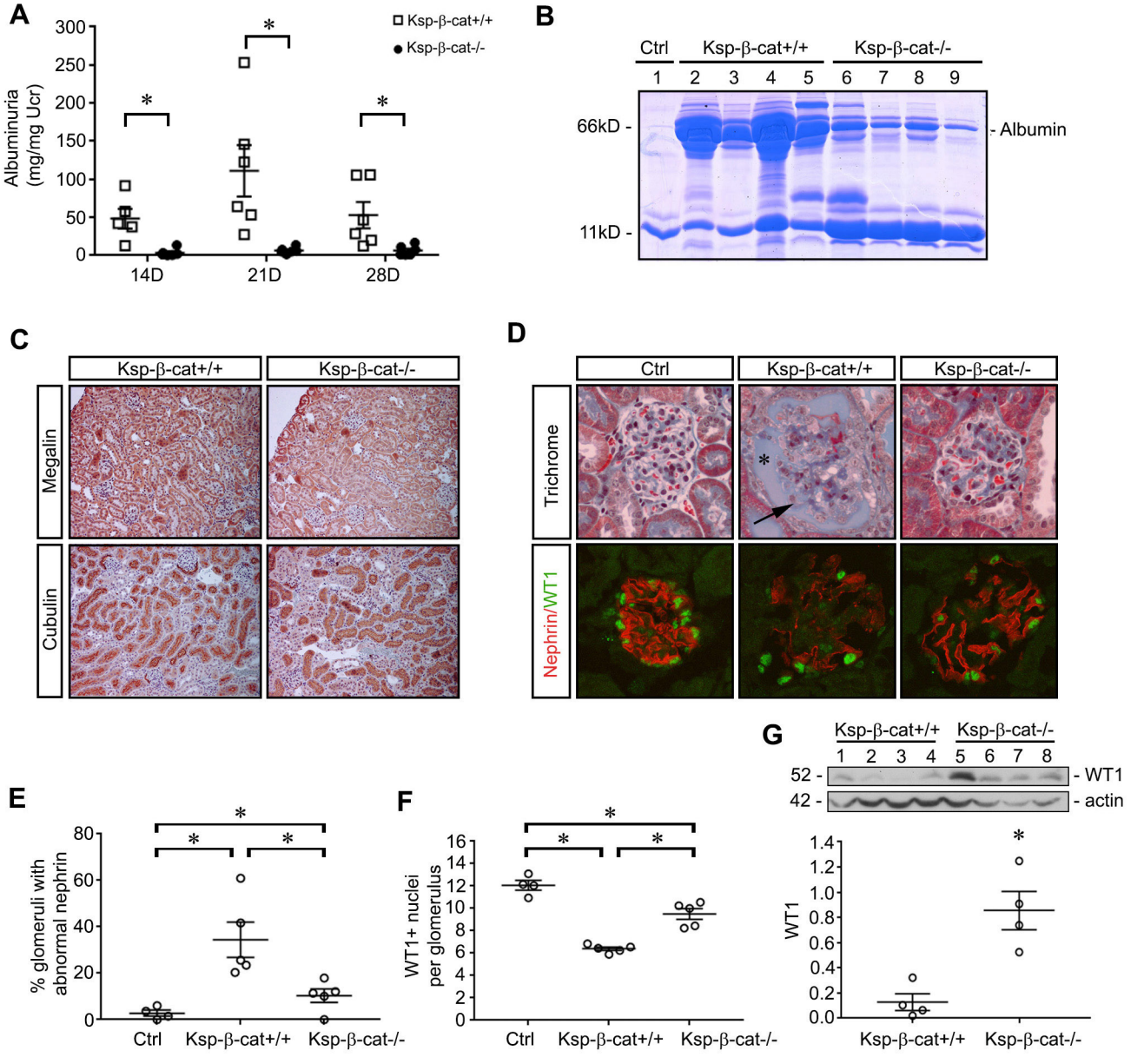

Figure 1. Tubule-specific β-catenin knockout mice are protected from glomerular injury. The β-cat-floxed mice (Ksp-β-cat+/+) and tubule-specific β-catenin knockouts (Ksp-β-cat-/-) were subjected to continuous angiotensin II (Ang II) infusions (1.5 mg/kg/day, osmotic minipump). (A) Urinary albumin excretion was measured in the Ksp-β-cat+/+ and Ksp-β-cat-/- mice (n=6) at 14, 21, and 28 days after Ang II infusion. * $P < 0.05$ compared to Ksp-β-cat+/+ at same timepoint, one-way ANOVA. (B) Gel electrophoresis of urine samples shows the composition of the protein excreted in the urine. Albumin is indicated. Urine from an untreated control mouse (Ctrl, lane 1) was included for reference. (C) Levels of megalin and cubulin are not different between Ksp-β-cat+/+ and Ksp-β-cat-/- mice after Ang II infusion. (D) Evaluation of glomerular histology reveals increased glomerular damage in the Ksp-β-cat+/+ compared to Ksp-β-cat-/- mice. Note the high levels of protein in Bowman's space in the Ksp-β-cat+/+ (asterisk), accompanied by significant glomerulosclerosis (arrow). In the Ksp-β-cat-/- mice overall glomerular injury including glomerulosclerosis was minimal. A control (Ctrl, untreated mouse) glomerulus is provided for reference. Immunofluorescence revealed significant disruption in nephrin and fewer WT1-positive podocytes in the Ksp-β-cat+/+ compared Ksp-β-cat-/- mice. (E) Quantitation of number of glomeruli with abnormal nephrin staining and (F) WT1-positive nuclei per glomeruli (n=5, *$P < 0.05$, one way ANOVA). (G) Immunoblot for WT1 showing depleted levels in the Ksp-β-cat+/+ mice, compared to Ksp-β-cat-/- mice. *$P < 0.05$, t-test.

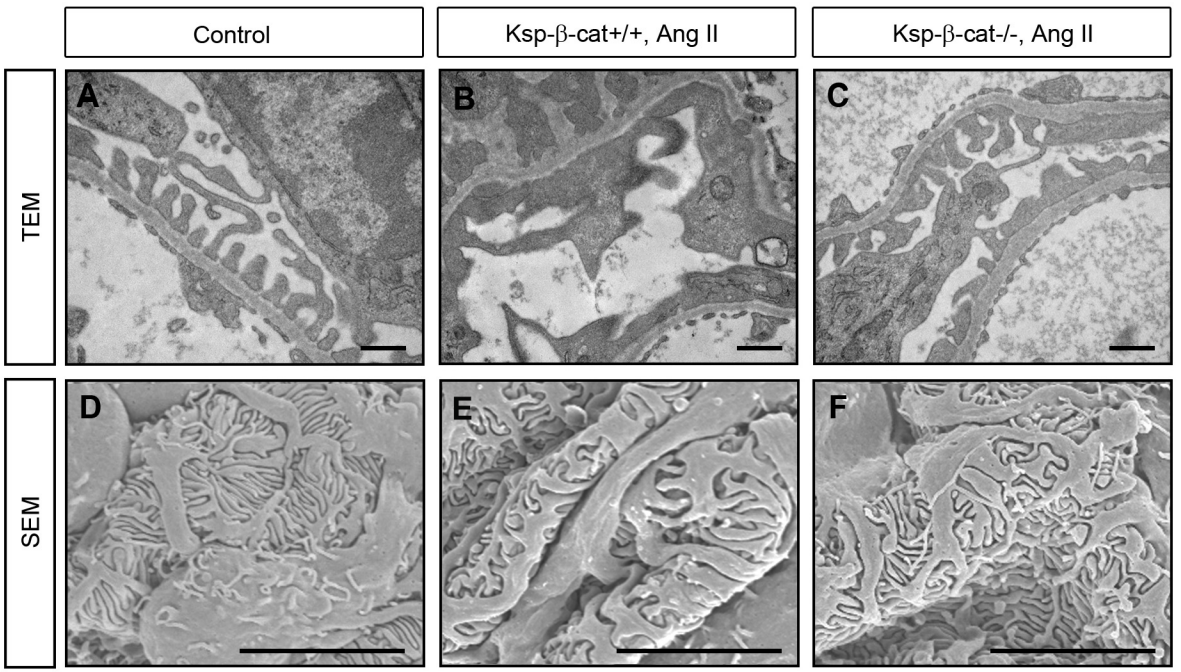

Figure 2. Podocyte foot process integrity is preserved in Ksp-β-cat-/- mice after Ang II infusion. Mice were treated as in Figure 1. (A-C) Transmission electron microscopy (TEM) showing extensive foot process effacement (arrows) in Ang II-treated Ksp-β-cat+/+ mice compared to Ksp-β-cat-/- mice. Bar equals 500 nm. (D-F) Scanning electron microscopy (SEM) revealed significant effacement in the control mice compared to untreated control and Ang II-treated Ksp-β-cat-/- mice. Bar equals 5 μm.

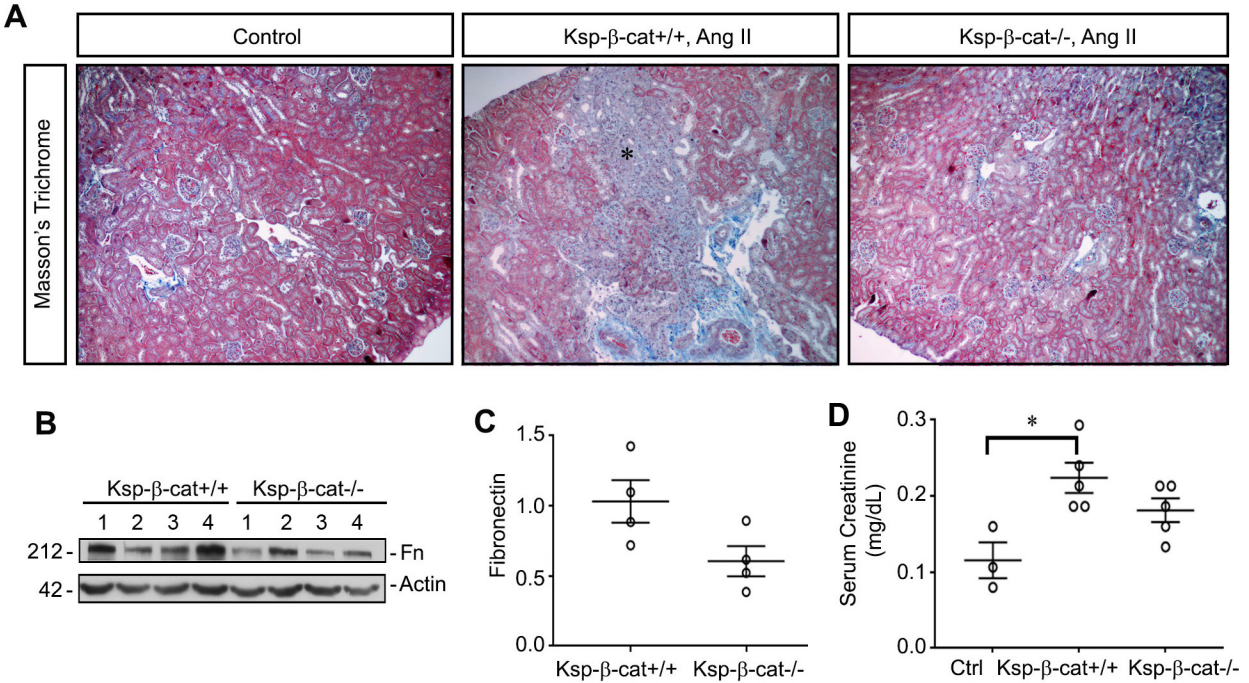

Figure 3. Ablation of β-catenin in renal tubules reduces interstitial fibrosis induced by Ang II infusion. (A) Masson's trichrome staining showing increased fibrosis in Ksp-β-cat+/+ mice after Ang II infusion (asterisk), compared to Ksp-β-cat-/- mice. (B) Western blots show a trend towards increased levels of fibronectin in the control mice, compared to Ksp-β-cat-/- mice (n=4). P = 0.06, t-test. (C) Measurement of serum creatinine shows that the only significant difference is observed between untreated control mice (Ctrl) and Ksp-β-cat+/+ mice, suggesting moderation of injury in the Ksp-β-cat-/- mice (n=5). * P < 0.05, one-way ANOVA.

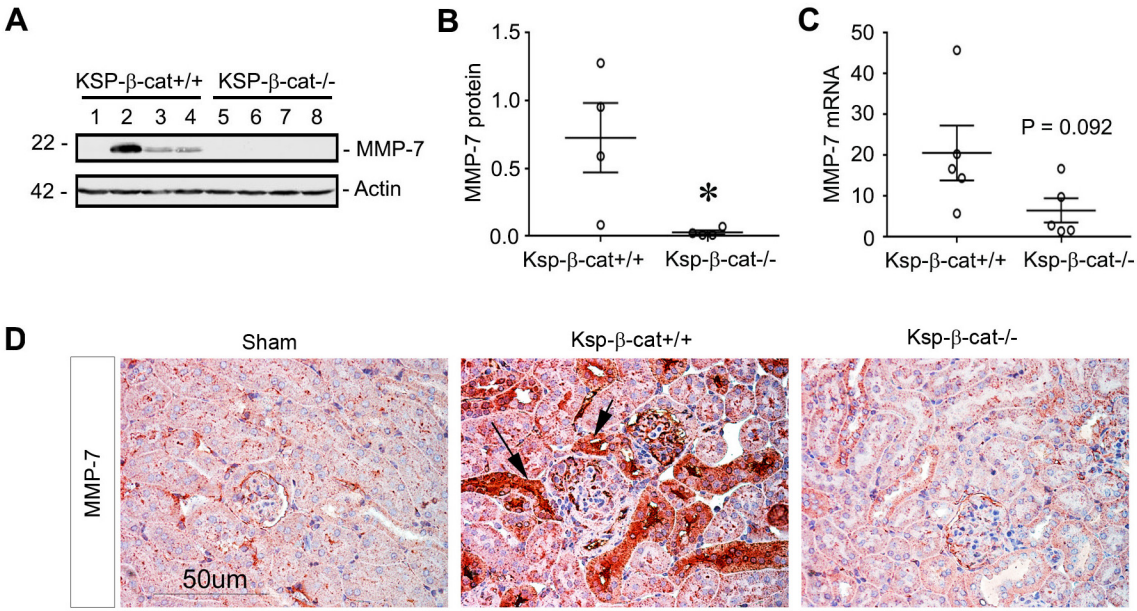

Figure 4. Renal expression of MMP-7 is reduced in Ksp-β-cat-/- mice after Ang II infusion. (A, B) Western blot analyses for MMP-7 reveal significant reduction in the Ksp-β-cat-/- mice after Ang II infusion, compared to Ksp-β-cat+/+ mice (n=4). Western blot (A) and quantitation after densitometry (B) are shown. *P < 0.05, t-test. (C) qRT-PCR shows a trend to higher expression of MMP-7 mRNA in the Ksp-β-cat+/+ mice as well (n=5, t-test). P = 0.092 two tailed, 0.046 one tailed. (D) Immunohistochemical staining for MMP-7 shows negligible staining in control mice, with dramatic upregulation in Ang II-treated Ksp-β-cat+/+ mice (arrows). A reduced MMP-7 staining was noticed in Ksp-β-cat-/- mice. Bar equals 50μM.

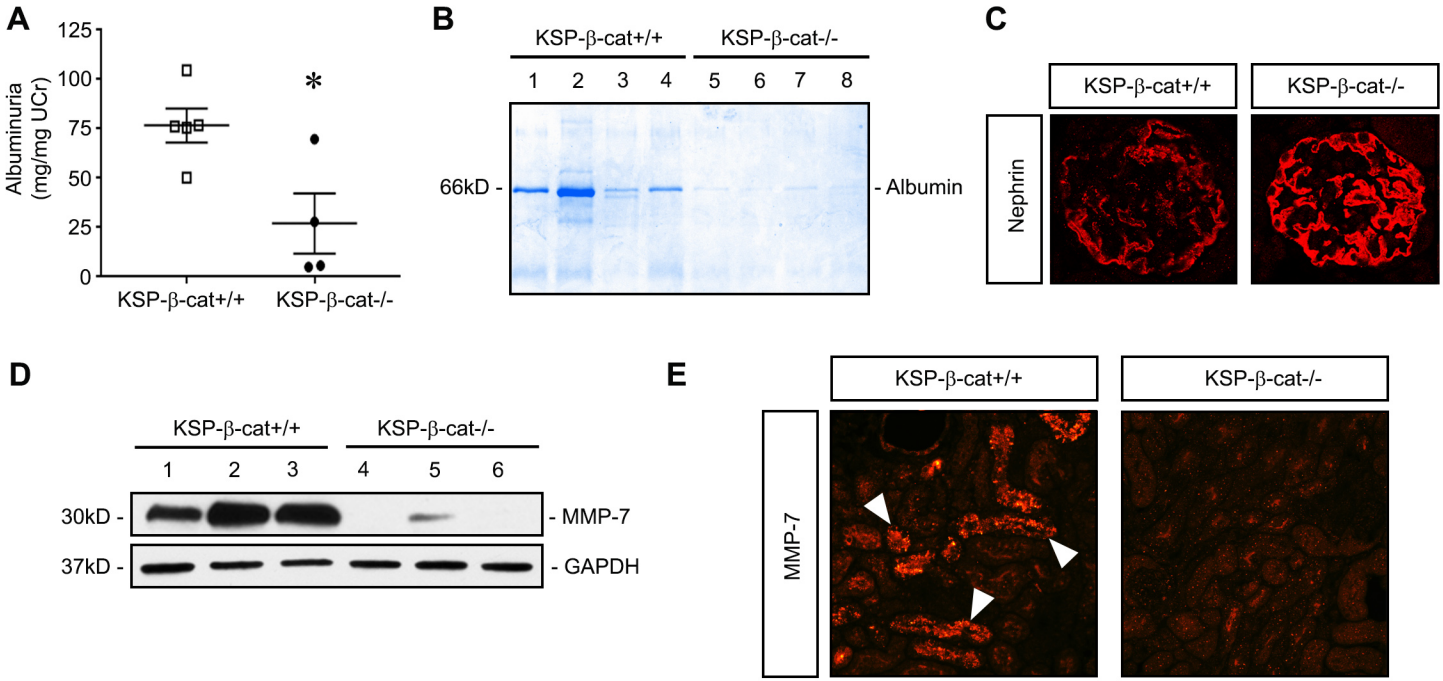

Figure 5. KSP-β-cat-/- mice are protected from adriamycin-induced kidney injury and proteinuria. (A) Urine albumin excretion 3 weeks after injection of adriamycin (22mg/kg) in KSP-β-cat+/+ compared to KSP-β-cat-/- mice (* $P < 0.05$, t-test). (B) Gel electrophoresis of urine samples showing reduction in albumin excretion in KSP-β-cat-/- mice. (C) Immunofluorescence showing greater nephrin disruption in KSP-β-cat+/+ mice. (D) Immunoblot demonstrating reduced kidney expression of MMP-7 in KSP-β-cat-/- mice. (E) Immunofluorescence for MMP-7 reveals strong upregulation in tubules from KSP-β-cat+/+ mice only.

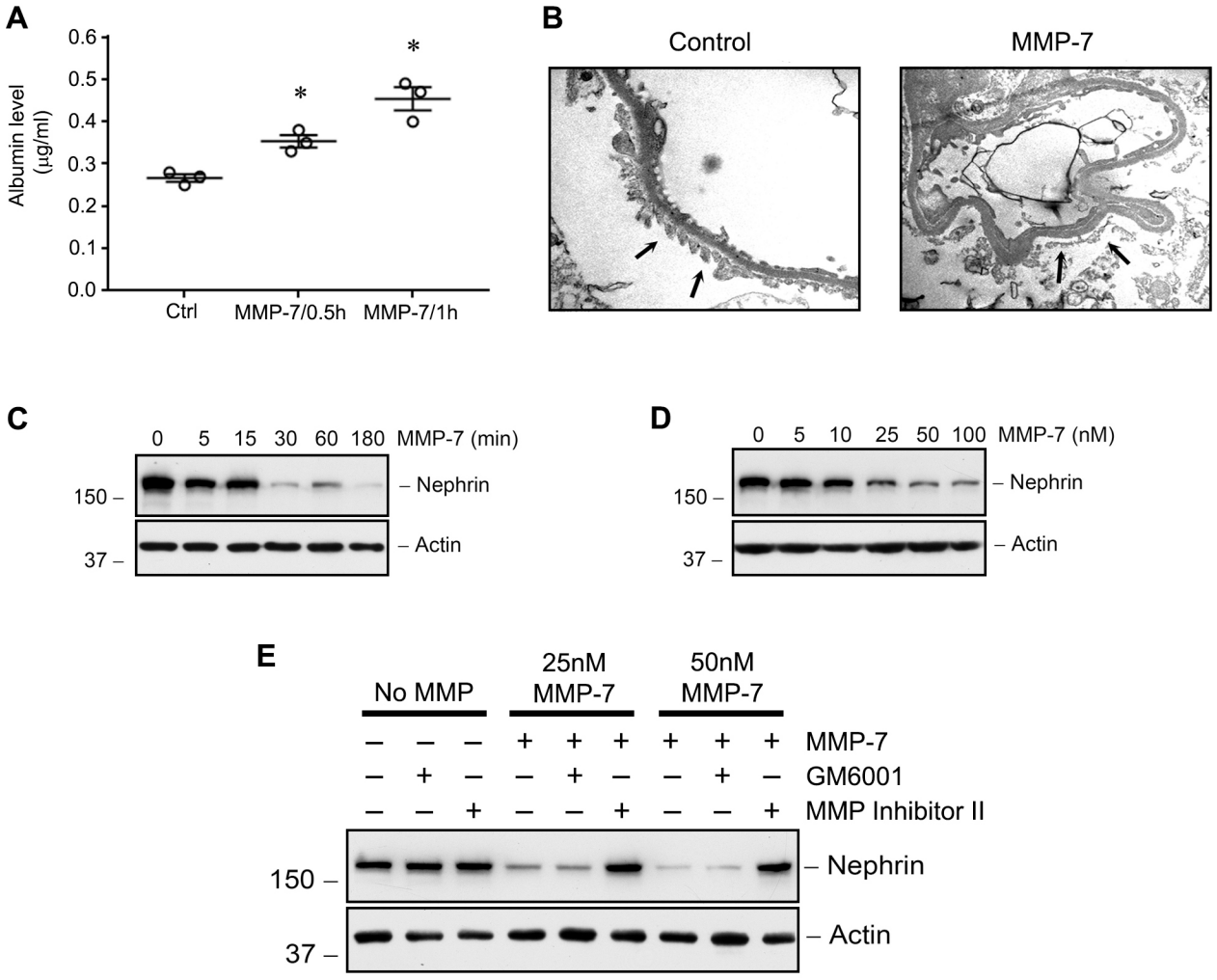

Figure 6. Recombinant MMP-7 decreases nephrin in a time- and dose-dependent manner in ex vivo glomeruli. (A) MMP-7 treatment (50 nM, 30 min) causes a significant time-dependent release of albumin from isolated rat glomeruli. *P < 0.05, repeated measures one way ANOVA. (B) TEM of isolated glomeruli shows flattening and fusion of foot processes in MMP-7-treated glomeruli compared to vehicle controls (arrows). In separate experiments, glomeruli were incubated with either the same concentration of MMP-7 (50 nM) for various periods of time (C) or with increasing amounts of MMP-7 for 60 minutes (D). Glomerular lysates were immunoblotted with antibodies against nephrin and actin. (E) Nephrin depletion by MMP-7 is dependent on its proteolytic activity. Rat glomeruli were pretreated with GM6001 (25 µM) or MMP inhibitor II (20 µM) for 30 minutes before incubation with MMP-7 (25 nM or 50 nM) for 60 minutes.

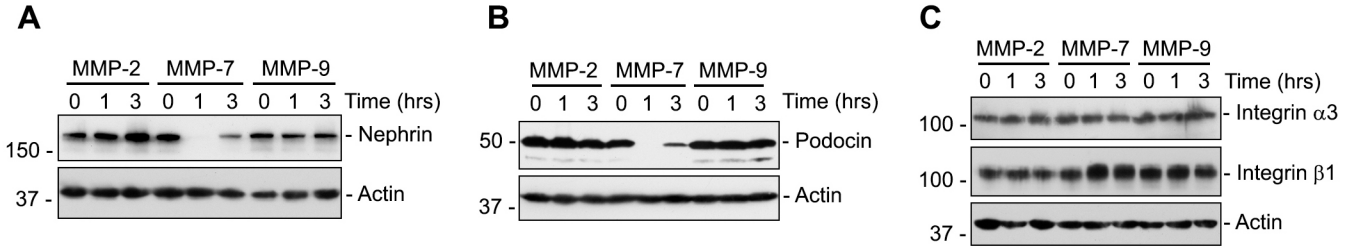

Figure 7. MMP-7 reduces nephrin and podocin levels in isolated glomeruli. (A) Rat glomeruli were incubated separately with MMP-2 (1 µg/ml, or 13.88 nM), MMP-7 (50 nM) and MMP-9 (1 µg/ml, or 10.9nM) and total protein immunoblotted for nephrin. Only MMP-7 was capable of reducing nephrin levels. (B) MMP-7 also reduces podocin protein in isolated glomeruli ex vivo. Glomerular lysates were immunoblotted with antibodies against podocin and actin. (C) MMP-7 does not affect other membrane proteins in podocytes such as integrin-α3 and integrin-β1. Western blot analyses of glomerular lysates reveal no effect on integrin-α3 and -β1 proteins after incubation with any of the three MMPs.

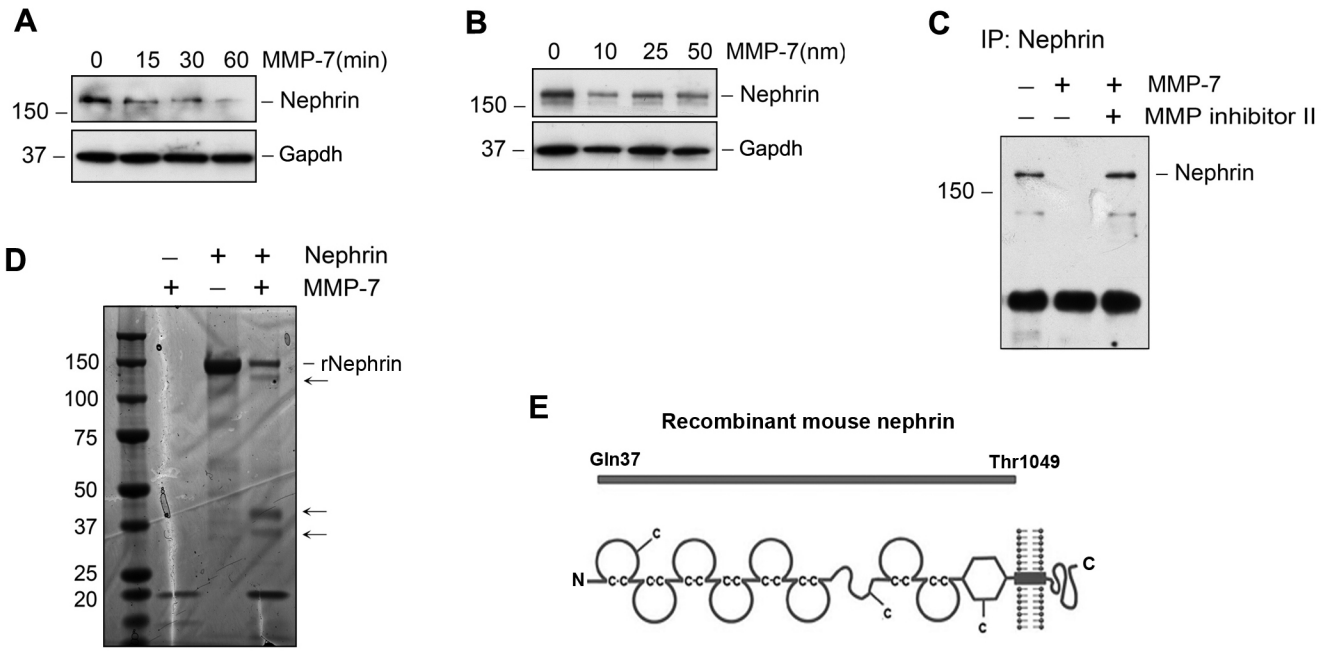

Figure 8. MMP-7 mediates nephrin degradation in vitro. (A, B) HEK-293 cells were transfected with nephrin expression vector for 48 hours, followed by incubation with MMP-7 (50 nM) for various periods of time (A) or with increasing amounts of MMP-7 for 60 minutes (B). (C) Nephrin from overexpressing cells was immunoprecipitated with anti-nephrin antibody, followed by various treatments as indicated. MMP-7 caused nephrin depletion, which was inhibited by MMP inhibitor II. (D, E) Representative SDS-PAGE shows that MMP-7 degrades recombinant mouse nephrin protein. Purified mouse nephrin protein (2 μg) was incubated with 50 nM MMP-7 for 60 minutes. Truncated form of mouse nephrin corresponding to Gln37 to Thr1049 (~150 kDa in size) is used (E). Arrows in Panel (D) indicate the degradation fragments of nephrin.

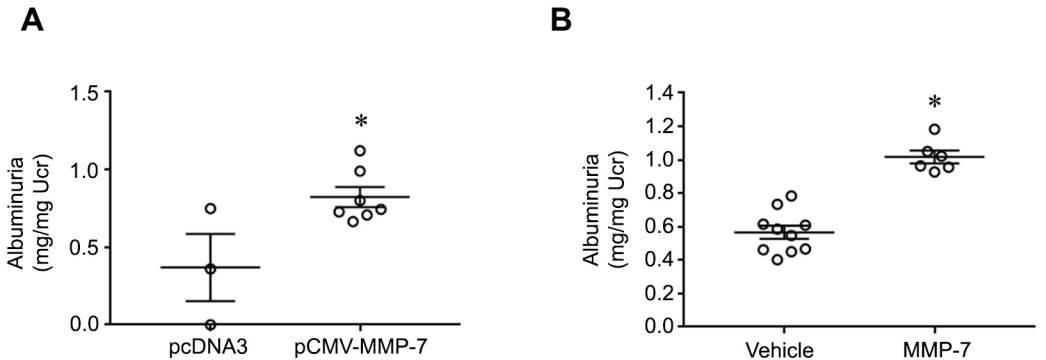

Figure 9. Delivery of MMP-7 gene or recombinant MMP-7 protein induces albuminuria in vivo. (A) Mice were injected intravenously with pcDNA3 or pCMV-MMP-7 vector (2 mg/kg), respectively. Urinary albumin concentration was assayed 24 h after injection. *P < 0.05 (n=7, t-test). (B) After injection with recombinant MMP-7 (1 mg/kg) for 3 hours, urinary albumin excretion was increased in the MMP-7-treated group, compared with vehicle controls. * P < 0.05 (n=6, t-test).

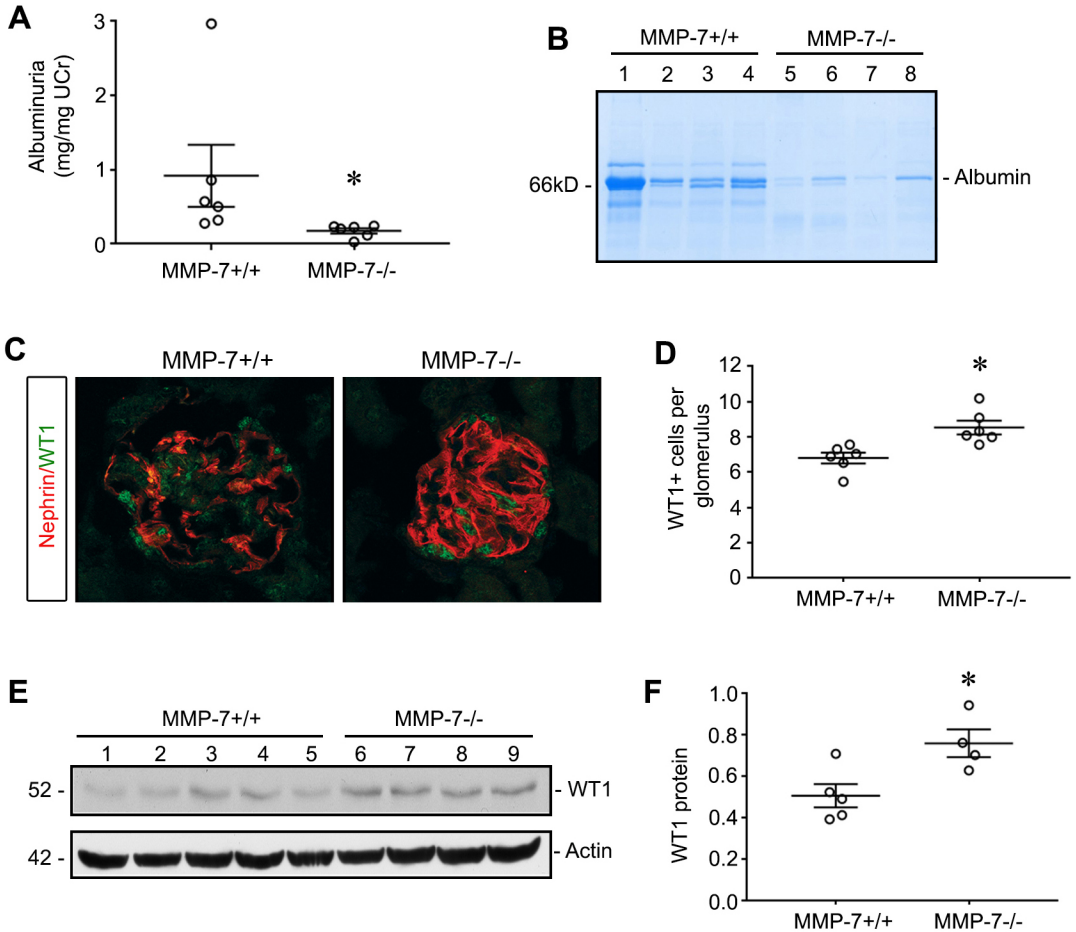

Figure 10. Mice with global ablation of MMP-7 are protected from Ang II-induced glomerular injury. Wild type (WT) and MMP-7-/- (KO) mice were treated with continuous infusions of Ang II (1.5 mg/kg/day). (A) Albuminuria is significantly reduced in the KO compared to WT mice. (B) Gel electrophoresis of urine samples demonstrate a reduced albumin excretion in MMP-7-/- mice, compared to MMP-7+/+ counterparts. (C) Immunofluorescence staining shows extensive nephrin disruption and a decrease in numbers of healthy WT1-positive podocytes in MMP-7+/+ mice. MMP-7 KO mice retained linear nephrin staining and numbers of WT1-positive nuclei. (D) Quantitation of WT1-positive nuclei per glomerulus (n=5-6, t-test). (E, F) Western blot analyses show an increased preservation of WT1 expression in MMP-7-/- mice after Ang II infusion, compared to MMP-7+/+ controls. Western blot (E) and quantitation (F) are shown. *P < 0.05 (n=4-5, t-test).